0273-2289/93/3940—0477$03.60

Axial Dispersion in a Liquid Fluidized Bed of Particles Akin to Immobilized Enzymes

GISELLA M. ZANIN,* IVO NEITZEL, AND FLAVIO F. DE MORAES

Maringa State University, Chemical Engineering Department 87020-900 Maringa, PR, Brazil

ABSTRACT

The axial dispersion of a liquid fluidized bed of controlled pore silica (CPS) particles has been determined by the pulse tracer method. The CPS used was the same as for enzyme immobilization, having an average diameter of 0.436 mm and mean pore size of 37.5 nm. The fluidization liquid is α-amylase liquefied manioc starch, 30% w/v, 45°C, pH=4.5. Nominal bed porosities tested were 0.7 and 0.8. The results show that the axial dispersion coefficient increases with greater superficial liquid velocities. Various available correlations tested disagree with each other to a large extent and are unable to represent collected experimental data.

Index Entries: Axial dispersion; fluidized bed; immobilized enzyme; controlled pore silica; liquefied starch.

NOMENCLATURE

C_t: tracer concentration at the reactor outlet, mg/cm³
D: axial dispersion coefficient, cm²/s
D_t: blue dextran molecular diffusion in the fluidizing solution 4.44×10^{-8} cm²/s (*12*)
D_0: axial dispersion coefficient for empty tubes, $D_0 = D_t + u^2 d_i^2 / (192 D_t)$, (*10*), cm²/s
d_i: reactor internal diameter, mm

*Author to whom all correspondence and reprint requests should be addressed.

d_p: average particle diameter, mm
E_t: residence time distribution, 1/s
E_θ: dimensionless E_t:$E_\theta = \bar{t}_R E_t$
g: gravitational acceleration, cm²/s
H_0: minimum fluidization bed height, mm
L: expanded bed height, mm
M_i: tracer injected mass, mg
M_s: fluidized solid total mass, g
n: Richardson and Zaki expansion index: $u/u_t = \epsilon^n$
P_e: mass transfer Peclet number
Q: defined by Eq. (8)
r: correlation coefficient
$R_\%$: percentage of recovered tracer relative to total mass injected
R_e: particle Reynolds number: $R_e = \rho\ u\ d_p/\mu$
R_{emf}: Reynolds number at minimum fluidization
t: sampling time, s
$\bar{t}_R$: mean residence time of the fluid inside the reactor, s
t_1: first moment of the reactor outlet tracer concentration distribution, s
u: fluidizing fluid superficial velocity, cm/s
u_i: fluidizing fluid intersticial velocity: $u_i = u/\epsilon$, cm/s
u_t: particle terminal velocity, cm/s
u_{mf}: minimum fluidization velocity, cm/s
v: fluidizing fluid volumetric flow rate, cm³/s
V_l: actual liquid volume in the reactor: $V_l = \epsilon\ V_T$, cm³
V_T: total bed volume: $V_T = \pi d_t^2 L/4$, cm³
ϵ: fluidized bed porosity: $\epsilon = 1 - M_s/\rho_s V_T$
θ: dimensionless time: $\theta = t/\bar{t}_R$
μ: fluidizing liquid viscosity, g/cm s
ν: kinematic viscosity, $\nu = \mu/\rho$, cm²/s
ρ: fluidizing liquid density, g/cm³
ρ_p: particle density, g/cm³
ρ_s: particle matrix density, g/cm³
ρ_{ap}: wet particle apparent density, g/cm³
σ^2: variance of the reactor outlet tracer concentration distribution, s²
σ_θ^2: dimensionless σ^2: $\sigma_\theta^2 = \sigma^2/t^2$
τ_e: space-time: $\tau_e = L/u_i = V_l/v$, s

INTRODUCTION

Fluidized-bed reactors have such advantages as uniform bed temperature, greater mass transfer, and easiness of handling suspended solid matter, and therefore find applications in several conventional catalytic and biotechnological processes (*1–4*). Within these reactors, the fluidized particles are free to move around and even set up whole-bed circulation depending on liquid flow distribution. Therefore, it is expected that the

axial dispersion of fluidized beds should be greater than for fixed beds. This should be of concern for lowering fluid-bed reactor conversion (*1,5*).

Very few authors (*6–9*) have developed correlations for the fluid axial dispersion in liquid fluidized beds that are applicable to the range of interest of immobilized enzyme reactors, that is: small particle size (viz. 0.5 mm), low particle density (1–1.5 g/cm^3), and very low liquid velocities ($R_e < 1$).

In this work, the axial dispersion of a liquid fluidized bed of controlled pore silica (CPS) particles was determined by the pulse tracer method (*10*). The reactor and particles were the same as used for immobilized enzyme reactor studies concerning the saccharification of liquefied manioc starch with immobilized glucoamylase (*11,12*). A previous paper (*13*) deals with the hydrodynamics of the same system regarding bed expansion and minimum fluidization parameters. Liquid dispersion experimental results will be compared with correlations for liquid and particle dispersion in fluidized beds.

Correlations for Liquid Axial Dispersion in Fluidized Beds

The available correlations for the axial dispersion of a fluidized bed will be described below.

Bruinzel et al. (*6*) propose:

$$(D/uL) = (d_p \cdot 10^3) / [L\,(4.3\,R_e^{0.18}\,\epsilon^{0.82})] \quad (1)$$

They have measured the axial dispersion using step tracer tests, with conductivity measurements at the following conditions:

- Column diameter (d_i): 10–100 mm;
- Expanded bed height (L): 300–1500 mm;
- Particle diameter (d_p): 0.05–0.50 mm; and
- Reynolds number (R_e): $0.64 < R_e/\epsilon < 16$.

Chung and Wen (*7*) have determined axial dispersion using fluorescein as tracer, injected as pulses or sine waves, and recording the response at two different heights in the fluidized bed. Their correlation is:

$$(D/uL) = (d_p\,\epsilon/L) / [(0.20 + 0.11\,R_e^{0.48})\,(R_{emf}/R_e)] \quad (2)$$

which was based on the following conditions:

- Column diameter (d_i): 50–102 mm;
- Expanded bed height (L): 600 mm;
- Particle diameter (d_p): 0.12–14.3 mm;
- Particle density (ρ_s): 1.52–11.3 g/cm^3;
- Liquid density (ρ): 1.00–10.2 g/cm^3;
- Reynolds number: $10^{-3} < R_e < 10^3$; and
- Bed porosity: $0.4 < \epsilon < 0.8$.

Chung and Wen (*7*) have shown that the application of their correlation to 482 data points from fixed and fluidized beds leads to an SD of 46%, which they consider satisfactory.

Krishnaswamy and Shemilt (*8*) offer the correlation:

$$(D/D_0) = 0.70\,(u_i/u_t)^{1.69} \tag{3}$$

which for 210 data points shows an SD of 17%. Its range of application is particle diameter (d_p): 0.31–6.4 mm and particle density (ρ_s): 1.28–11.3 g/cm^3.

Krishnaswamy et al. (*9*) have introduced a new correlation:

$$(D/u_iL) = (1 - 0.74/\epsilon^{0.25})^2/2 \tag{4}$$

which adjusted 314 data points from different works with an SD of 8.0%. Recommended range of application is:

- Particle size (d_p): 0.5–14.3 mm;
- Particle density (ρ_s): 1.28–11.3 g/cm^3; and
- Bed porosity (ϵ): $\epsilon < 0.95$.

As observed by Metha and Shemilt (*14*), fluid-bed liquid dispersion may depend on: size and shape of the particles, difference of density between particle and liquid, liquid velocity, column size, and bed height. Some dependent variables, such as bed porosity, particle terminal velocity, and Reynolds number, are used in the correlations Eqs. (1)–(4). Eq. (3) additionally uses the coefficient of axial liquid dispersion in the unpacked column (D_0), which is justified by the authors, as a way to introduce the effects of column diameter and liquid radial velocity profile.

Correlations for Particle Axial Dispersion in Fluidized Beds

Some recent correlations, developed for particle axial dispersion shall be used also for comparison. They are owing to work by Martin and Van der Meer (Eq. 5), van der Meer et al. (Eq. 6), van der Meer and Wesseling (Eq. 7), and were collected by van der Meer and Wesseling (*15*):

$$D = 0.04\,u^{1.8}\ (\text{m}^2/\text{s}), \qquad r = 0.93 \tag{5}$$

applicable to: $0.5 < \epsilon < 0.9$ and $2 < u < 20$ mm/s, r being the correlation coefficient.

$$(D/\nu) = 70\,[u/(g^{1/3}\nu^{1/3})]^{2.3} \tag{6}$$

$$D = 0.123\,u^{1.98}\ (\text{m}^2/\text{s}), \qquad r = 0.97 \tag{7}$$

applicable to: $0.5 < \epsilon < 0.9$ and $2 < u < 600$ mm/s.

MATERIALS

The CPS used was acquired from Corning Glass Works—USA having the following characteristics (*12*): average particle diameter (d_p): 0.436 mm; mean pore size; 37.5 nm; internal particle porosity: 0.566; particle matrix density (ρ_s): 2.178 g/cm^3; particle density (dry) (ρ_p): 0.948 g/cm^3; apparent wet particle density (pores filled with fluidizing liquid) (ρ_{ap}): 1.563 g/cm^3. Blue-dextran, mol wt 2,000,000 was used as the tracer dye in a concentration of 52 mg/mL, and the output dye concentration was measured with a spectrophotometer Micronal B-280, set to 625 nm. Reactor design, dimensions, and other details are shown in Fig. 1.

The fluidizing liquid was α-amylase preliquified manioc starch, 30% w/v, 45°C, pH=4.5, prepared by the method described by Zanin and Moraes (*12,17*). Its physical properties were (*12,17*): $\rho = 1.101$ g/cm^3, $\mu = 2.344$ cp. The CPS fluidized with this liquefied starch solution has given the following experimental parameters (*11*): minimum fluidization velocity: $u_{mf} = 2.13 \times 10^{-2}$ cm/s; particle terminal velocity: $u_t = 3.00$ cm/s; Richardson and Zaki expansion index: $n = 5.746$.

METHODS

Liquid axial dispersion in the fluidized-bed reactor was determined by injecting pulses of the tracer dye just below the liquid distributor and collecting liquid samples at the reactor outlet, in 10-s intervals. Actual mass (M_i) of the injected dye was determined by weight measurements of the syringe before and after injection.

Before each test, a new particle batch was submitted to vacuum for 10 min, and then the fluidizing liquid was added slowly under vacuum, so as to fill up the particle pores totally. These particles were loaded in the reactor, which was operated for 20 min, to guarantee thermal and hydrodynamic equilibrium. Tests conditions are shown in Table 1.

RESULTS

Tracer concentration distribution as a function of time is shown in Figs. 2 and 3. The axial dispersion number and Peclet ($D/u\ L = 1/P_e$), shown in Table 1, have been calculated from the first (t_1) and second (σ^2) moments of the outlet tracer concentration distribution (C_t) (*10*), as follows:

$$Q = \int_0^\infty C_t dt, \qquad C_1 = C_t/Q \tag{8}$$

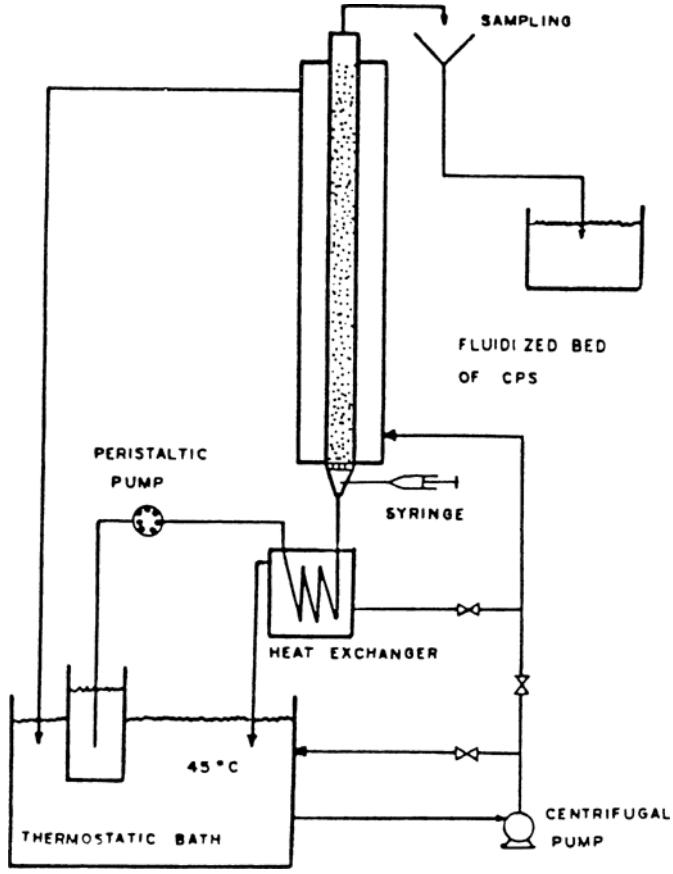

Fig. 1. Fluidized-bed reactor setup for studying axial fluid dispersion. Column internal diameter: 8.04 mm. Maximum bed height: 760 mm. Material of construction is Plexiglas™. Reactor temperature (45°C) and isothermicity are maintained with the aid of an external water jacket and thermostatic bath, which is automatically controlled. A mesh of stainless steel, size 100, was used as liquid distributor. The reactor was operated as a "closed" system at both ends, in the sense of Levenspiel and Bischoff (*16*).

$$t_1 = \int_0^\infty t\, C_1\, dt \tag{9}$$

$$\sigma^2 = \int_0^\infty t^2\, C_1\, dt - t_1^2 \tag{10}$$

$$t_1/\tau_e = 1 \tag{11}$$

$$\sigma^2/\tau_e^2 = (2/P_e)\{1 - [1 - \exp(-P_e)]/P_e\} \tag{12}$$

The mean residence time ($\bar{t}_R$) of the fluid inside the reactor is equal to t_1 given by Eq. (9), since the reactor experimental setup follows the "closed" model (*16*). Hence, $\bar{t}_R$ should be equal to τ_e (space-time $= V_l/v$). Table 1 compares results for $\bar{t}_R$ and τ_e.

Table 1
Tracer Test Experimental Conditions and Calculated Parameters

Bed porosity, ϵ	0.752		0.801		
Test	1	2	1	2	3
CPS mass (g)	10.45	10.45	6.97	6.97	6.97
Superficial velocity (cm/s)	0.154	0.157	0.349	0.354	0.410
Initial bed height (cm)	39.9	39.9	27.0	27.0	27.0
Expanded bed height (cm)	73	73	73	73	73
Mean residence time (s)	326.4	374.4	187.8	168.0	148.8
Space time, τ_e (s)	356.4	349.2	167.4	165.6	142.8
Mass of transfer injected (mg)	22.64	21.64	23.49	26.99	21.86
Recovered tracer (%)	83.68	96.64	85.66	80.36	89.92
σ_θ^2	0.049297	0.058720	0.052497	0.036128	0.041226
Dispersion number (D/uL)	0.0253	0.0303	0.0280	0.0184	0.0229

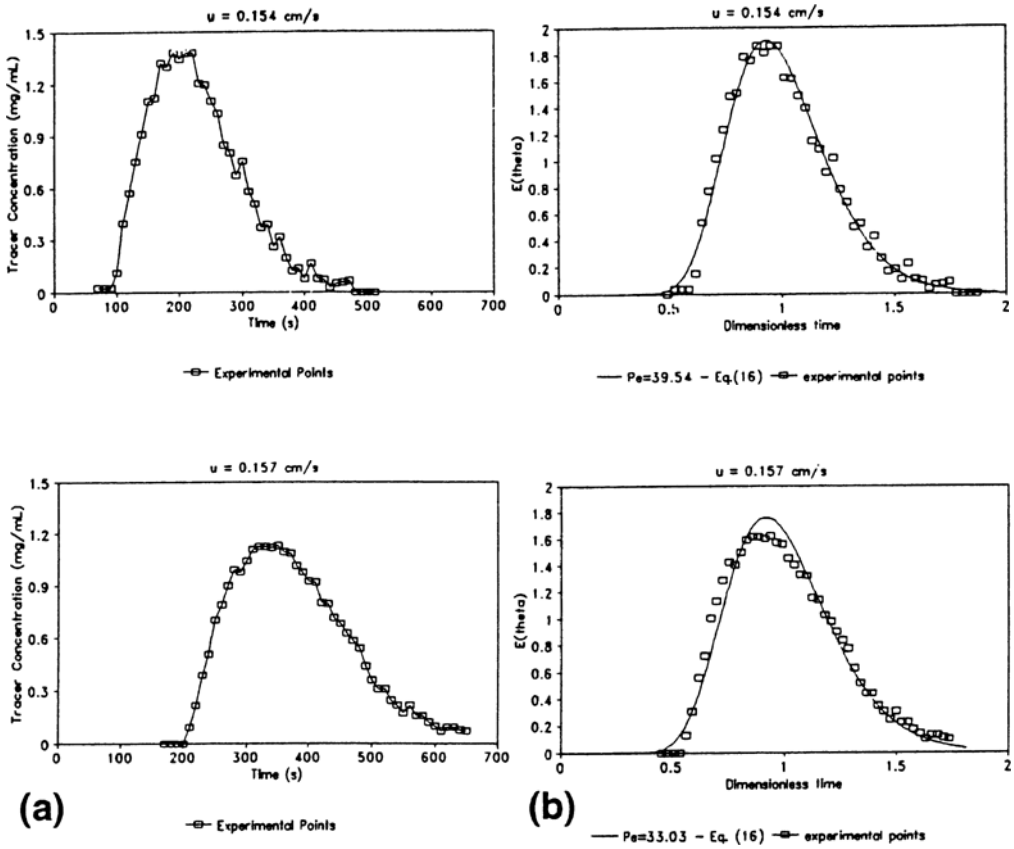

Fig. 2. (a) Results of the pulse tracer tests. (b) Comparison of the experimental data with theoretical curves for the residence time distribution of a tubular reactor with axial dispersion. $\epsilon = 0.752$, $H_0 = 399$ mm, $L = 730$ mm, $V_l = 27.87$ cm^3, $M_s = 10.45$ g.

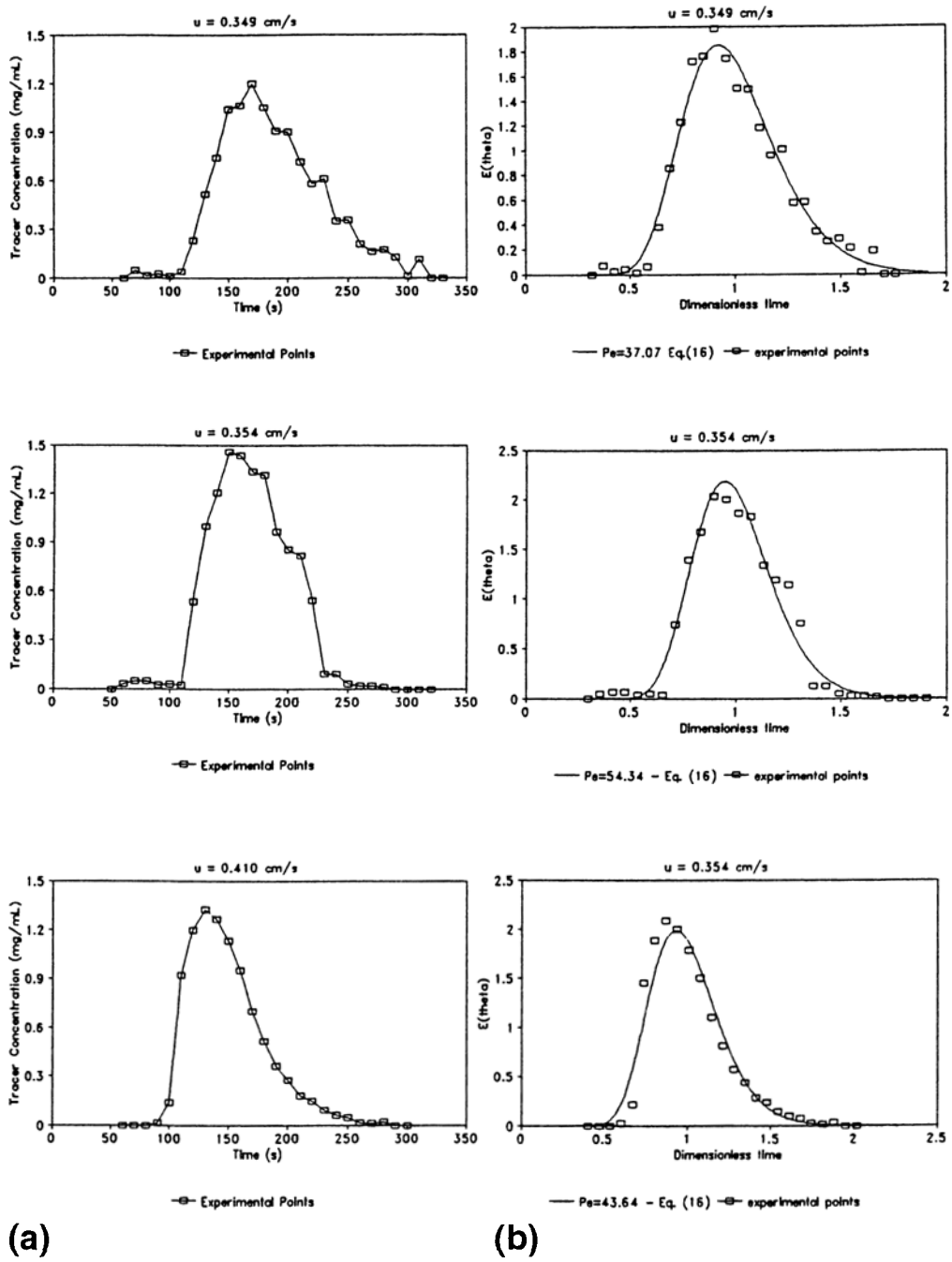

Fig. 3. (a) Results of the pulse tracer tests. (b) Comparison of the experimental data with theoretical curves for the residence time distribution of a tubular reactor with the axial dispersion. $\epsilon = 0.801$, $H_0 = 270$ mm, $L = 730$ mm, $V_I = 29.69$ cm^3, $M_s = 6.97$ g.

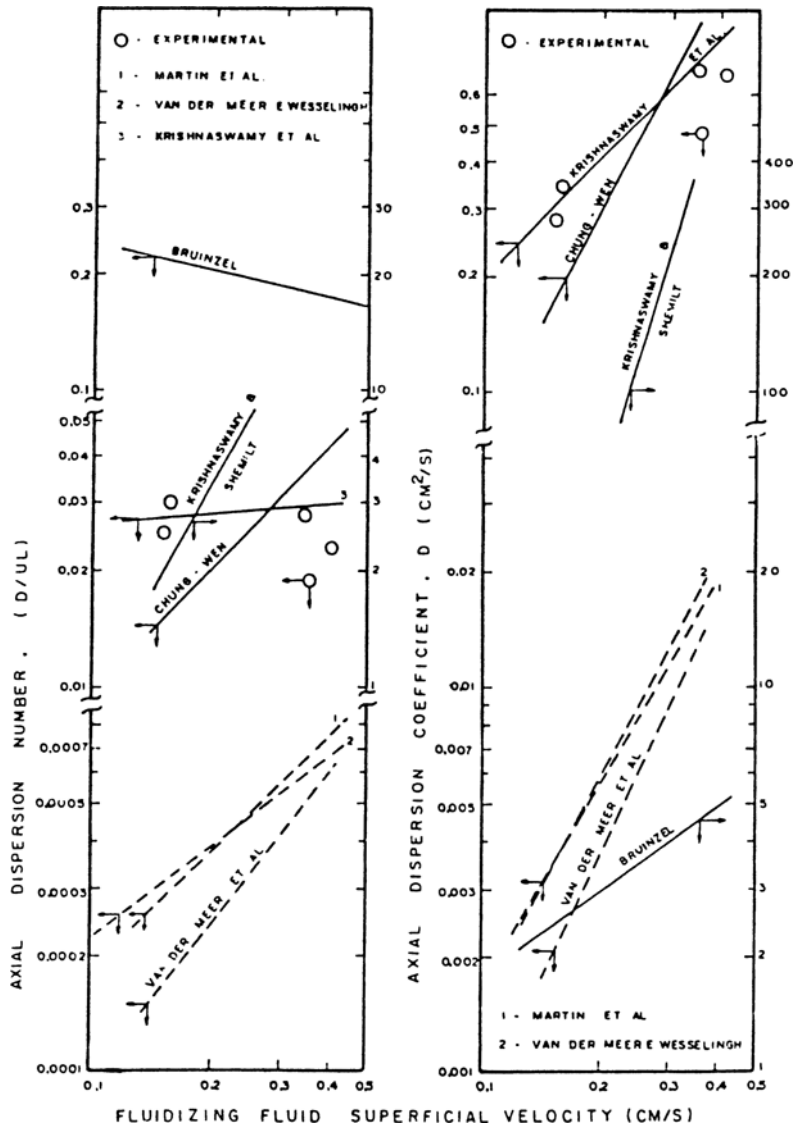

Fig. 4. Comparison between the experimentally determined axial dispersion number (D/uL) and dispersion coefficient (D) with predicted values given by the correlations, Eqs. (1)–(7). _____ Fluid dispersion; - - - - particle dispersion.

Tracer recovery at the outlet is calculated by:

$$R_{\%} = (v\,Q/M_i) \times 100 \tag{13}$$

Table 1 shows the experimental values obtained for tracer recovery.

Dispersion number is plotted in Fig. 4 as a function of liquid superficial velocity. Experimental and predicted values, the latter calculated with correlations, Eqs. (1)–(4), are compared. Although the correlations, Eqs.

(5)–(7), are for particle dispersion rather than liquid dispersion, they have also been used for comparison.

DISCUSSION

Residence Time Distribution

The analysis of Figs. 2 and 3 definitely shows that the fluidized-bed reactor does not behave as an ideal tubular flow reactor (PFR). There is a clear spreading of the fluid residence time, accompanied by early appearance of the concentration peak. This can be related to backmixing or channeling (*10*). Channeling could be the result of inhomogenities at the fluid distributor or imperfect sealing at its rim, whereas the wavy aspect of the outlet tracer concentration in Fig. 3 suggests that there is an overall fluid recirculation in the bed (*10*). Similar results have been observed when starch solution was 1.6% w/v, and glucose was used as tracer (*18*).

Theoretical residence time distribution given by the model of tubular reactor with axial dispersion and "closed" boundaries (*10*) was calculated with the following equations (*19,20*). For $P_e < 20$:

$$E_\theta = \exp(Pe/2) \sum_{i=1}^{\infty} (-1)^{i+1} 8\,\alpha_i^2 / (4\,\alpha_i^2 + 4\,P_e + P_e^2)$$

$$\exp\{-[(4\,\alpha_i^2 + P_e^2)/4\,P_e)]\,\theta\} \qquad (14)$$

where $\alpha_{2n-1} = \beta_n$ and $\alpha_{2n} = \gamma_n$, $n = 1,2\ldots$, with β_n and γ_n taken as the roots in ascending order of the equations:

$$(\beta/2)\,tg(\beta/2) - P_e/4 = 0,\ (\gamma/2)\,cot(\gamma/2) + P_e/4 = 0 \qquad (15)$$

Eq. (14) is in fact valid for any value of Peclet; however, it is recommended for $P_e < 20$ because it converges slowly for greater P_e values. For $P_e > 20$:

$$E_\theta = 2\,(P_e / \pi\,\theta)]^{1/2} \exp[-(P_e / 4\,\theta)\,(1 - \theta)^2]\,[1 + (P_e\,\theta / 2)] - 2P_e\,[1 + (P_e / 4)\,(1 + \theta)] \exp(P_e)\,erfc\,[(P_e / 4\,\theta)]^{1/2}\,(1 + \theta) \qquad (16)$$

Equation (16), recommended for $P_e > 20$, is obtained by derivation and multiplication by (-1) of Brenner's (*20*) asymptotic solution for the reactor response to a negative step tracer input. Since a pulse test was used, the reactor outlet tracer concentration represents the experimental residence time distribution (*10*). This is compared in Figs. 2 and 3, part b with the theoretical Eqs. (14) and (16). Peclet values used for plotting were obtained as indicated in the previous section. The good agreement between theoretical and experimental residence time distribution supports the validity of applying the axial dispersion model to liquid fluidized beds.

Mean Residence Time and Tracer Recovery

Table 1 shows a good agreement between mean residence time ($\bar{t}_R = t_1$) calculated by Eq. (9) and the space-time (τ_e). Small discrepancies are considered to be within the experimental errors expected for this type of test. Tracer recovery has varied within 80–97%, although no visible adsorption in the reactor walls or exterior of the particles was seen. The high molecular weight chosen for the dye should have prevented adsorption inside the particle pores. Therefore, lower than 100% tracer recovery might be associated with some interference in the analytic method.

Fluid Axial Dispersion

Figure 4 shows general disagreement among the various proposed correlations for axial dispersion when applied to the conditions of this work. All correlations, however, predict an increase in dispersion number with an increase in the liquid superficial velocity, except Eq. (1) resulting from the work of Bruinzel et al. (*6*). Emery and Cardoso (*21*) have already noted this opposite trend of Eq. (1) when applied to their own data.

Figure 5 compares predicted values with experimental results for 20 data points, including data from this work and several authors. Agreement is also poor. These differences may be owing to the fact that most correlations were developed with a bias for larger and denser particles.

Given the interest in fluidized-bed applications in biotechnology, the need to develop an appropriate correlation to be used with small particles and low liquid velocities seems warranted.

Particle Dispersion

Correlations for particle dispersions, Eqs. (5)–(7) predict values that are two orders of magnitude lower than actual fluid dispersion values. Therefore, it can be concluded that particle movement in the liquid fluidized bed does not contribute significantly to axial fluid dispersion.

CONCLUSIONS

1. The fluidized axial dispersion in a liquid fluidized bed of small particles, akin to immobilized enzyme applications, has shown an intermediate level of mixing.
2. An increase in flow rate increases both fluid and particle axial dispersion; however, the latter is two orders of magnitude lower in value.
3. The fluid residence time distribution in this liquid fluidized bed is satisfactorily represented by the model of a tubular reactor with axial dispersion and "closed" boundaries.

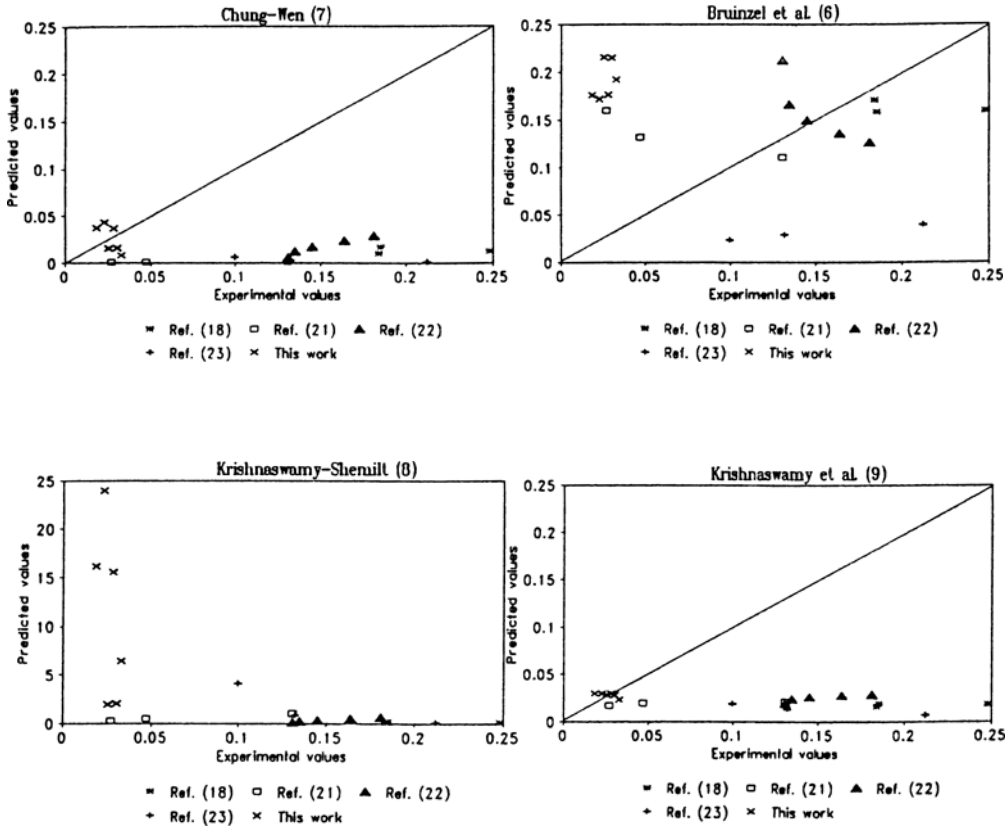

Fig. 5. Comparison between predicted and experimental axial dispersion data.

4. Available correlations disagree with each other to a large extent and are unable to represent collected dispersion data. Therefore, considering the potential applications of immobilized enzymes, the development of a suitable correlation seems warranted.

ACKNOWLEDGMENTS

This work was supported by FINEP and Maringa State University.

REFERENCES

1. Burli, A. B., Senthilnathan, P. R., and Subramanian, N. (1979), *Can. J. Chem. Eng.* **57**, 648–650.
2. Busche, R. M. and Allen, B. R. (1989), *Appl. Biochem. Biotechnol.* **20–21**, 357–374.

3. Andrews, G. F. and Fonta, J. P. (1989), *Appl. Biochem. Biotechnol.* **20–21,** 375–390.
4. Davidson, J. F., Clift, R., and Harrison, D. (1985), *Fluidization,* 2nd ed., Academic, London.
5. Wen, C. Y. and Fan, L. S. (1973), *Chem. Eng. Sci.* **28,** 1768–1772.
6. Bruinzel, C., Reman, G. H., and van der Laan, E. T. H. (1960), *Proceedings of the Symposium on Interaction between Fluids and Particles,* Institute of Chemical Engineering, London, 136.
7. Chung, S. F. and Wen, C. Y. (1968), *AIChE. J.* **14,** 857–866.
8. Krishnaswamy, P. R. and Shemilt, L. W. (1972), *Can. J. Chem. Eng.* **50,** 419,420.
9. Krishnaswamy, P. R., Ganapathy, R., and Shemilt, L. W. (1978), *Can. J. Chem. Eng.* **56,** 550–553.
10. Levenspiel, O. (1972), in *Chemical Reaction Engineering,* 2nd ed., John Wiley & Sons, New York, Chapter 9, pp. 253–325.
11. Zanin, G. M., Kambara, L. M., Calsavara, L. P. V., and de Moraes, F. F. (1988), *Proceedings of XVI Encontro sobre Escoamento em Meios Porosos* **I,** 234–252.
12. Zanin, G. M. (1989), Sacarificacao de Amido em Reator de Leito Fluidizado com Enzima Amiloglicosidase Imobilizada. Ph.D. Thesis, Faculdade de Engenharia de Alimentos, Universidade Estadual de Campinas, Campinas-SP, Brasil.
13. Zanin, G. M. and de Moraes, F. F. (1984), *Proceedings of XII Encontro sobre Escoamento em Meios Porosos* Maringa, **I,** 267–285.
14. Metha, S. C. and Shemilt, L. W. (1976), *Can. J. Chem. Eng.* **54,** 43–51.
15. van der Meer, A. P. and Wesselingh, J. A. (1986), in *Heat and Mass Transfer in Fixed and Fluidized Beds,* van Swaaij, W. P. M. and Afgan, N. H., eds., Springer-Verlag, Berlin, pp. 601–613.
16. Levenspiel, O. and Bischoff, K. B. (1963), *Adv. Chem. Eng.* **4,** 95–198.
17. Zanin, G. M. and de Moraes, F. F. (1989), *Revista de Microbiologia* **20(3),** 367–371.
18. Zanin, G. M. and de Moraes, F. F. (1983), *Revista Brasileira de Engenharia Quimica* **7,** 47–58.
19. Froment, G. F. and Bischoff, K. B. (1990), in *Chemical Reactor Analysis and Design,* 2nd ed., John Wiley and Sons, New York, p. 530.
20. Brenner, H. (1962), *Chem. Eng. Sci.* **17,** 229–243.
21. Emery, A. N. and Cardoso, J. P. (1978), *Biotechnol. Bioeng.* **20,** 1903–1929.
22. Cabral, J. M. S. (1982), Estudos de Imobilizacao de Enzimas pelo Metodo dos Metais de Transicao, Ph.D. Thesis, Universidade Tecnica de Lisboa.
23. Zanin, G. M. and de Moraes, F. F. (1983), *Proceedings of XI Encontro sobre Escoamento em Meios Porosos,* Rio de Janeiro, **II,** 64–82.